Possible onset of multifaceted excitation modes in ^{29}Al

H. Sultana,[1] R. Bhattacharjee,[2] A. Chakraborty,[1,*] M. A. Khan,[3] S. S. Bhattacharjee,[2,†] R. Chakrabarti,[4] S. Das,[2] U. Garg,[5] S. S. Ghugre,[2] R. Palit,[6] R. Raut,[2] S. Saha,[6] S. Samanta,[2] J. Sethi,[6] A. K. Sinha,[7] and T. Trivedi[8]

[1]*Department of Physics, Siksha Bhavana, Visva-Bharati University, Santiniketan, West Bengal 731 235, India*
[2]*UGC-DAE Consortium for Scientific Research, Kolkata Centre, III/LB-8, Bidhan Nagar, Kolkata 700 098, India*
[3]*Department of Physics, Aliah University, IIA/27, Newtown, Kolkata 700 156, India*
[4]*Department of Physics, University of Mumbai, Vidyanagari, Mumbai 400 098, India*
[5]*Department of Physics, University of Notre Dame, Notre Dame, Indiana 46556, USA*
[6]*Tata Institute of Fundamental Research, Mumbai 400 005, India*
[7]*UGC-DAE Consortium for Scientific Research, Indore 452 017, India*
[8]*Guru Ghasidas University, Bilaspur 495 009, India*

(Received 1 May 2018; revised manuscript received 21 June 2018; published 31 July 2018)

This paper reports on an investigation on the level structure of the odd-mass ^{29}Al nucleus populated via heavy-ion induced fusion evaporation reaction. Rotational sequences with fast magnetic dipole transitions have been identified. These sequences exhibit the essential characteristic features of magnetic-rotation-like behavior, which has been corroborated through lifetime measurements using the Doppler shift attenuation method. The sequences also show features exhibited by axially deformed nuclei. Thus, the level structure presents the possibility of existence of multifaceted excitation modes in ^{29}Al, which are believed to be the first of its kind observed in the $A \approx 30$ region. Shell model calculations, carried out within the *sd*-model space, qualitatively reproduce the experimental observations.

DOI: 10.1103/PhysRevC.98.014330

I. INTRODUCTION

Nuclei belonging to the middle and the upper part of the *sd*-shell region have been extensively investigated over the past few decades. Among the odd-mass *sd*-shell nuclei, ^{29}Al is one of the cases where spectroscopic information related to its level structure is still scarce. Experimental studies on the level structure of ^{29}Al were previously undertaken by various groups using a variety of probes. β^--decay studies of ^{29}Mg [1–3] could populate the excited levels of ^{29}Al up to the excitation energy of 4.4 MeV. Because of $J^\pi = 3/2^+$ of the ground state of the parent ^{29}Mg, these studies could observe levels in ^{29}Al between spins 1/2 and 7/2. Further, these β-decay experiments could establish only the possible allowed range of spin values for a majority of the observed excited levels, leaving many ambiguities in the spin-parity assignments of the levels. Experiments were also carried out using the ^{26}Mg(α, p)^{29}Al reaction. These studies could extend the level structure of ^{29}Al up to $E_x \approx 7$ MeV. Detailed angular correlation and polarization measurements were also carried out using Ge(Li) and NaI detectors [4,5] and the unambiguous spin-parity assignments were made for many of the excited levels. Lifetime measurements in the few-femto-second regime were also carried out for a majority of the observed levels by using the Doppler shift attenuation method (DSAM) [6,7]. The experimental findings from these measurements could provide the necessary testing ground for the shell model predictions in the valence *sd*-model space [8,9]. Spectroscopic investigation on ^{29}Al was also carried out by using proton pickup reactions such as ^{30}Si(t, α) [10] and ^{30}Si(d, ^{3}He) [11]. The levels up to $E_x \approx 5$ MeV could be established from these studies. The spectroscopic strengths for majority of the positive-parity states were measured and compared with the prediction of the truncated shell-model calculations using *sd* basis space and modified surface delta interaction. Thus, till now the available information on the level structure of ^{29}Al has primarily been deduced from the decay studies and light-ion induced reactions. The only available spectroscopic work for ^{29}Al involving heavy ion induced fusion-evaporation reaction is that from the recent study of Dungan *et al.* [12].

It is worthwhile mentioning that the nuclei in $A \approx 30$ region occupy the *sd*-valence orbitals outside the ^{16}O core. This is a unique region in that there are sufficient number of valence nucleons which could favor the onset of collectivity in the immediate neighborhood of the $N = Z = 8$ shell closure and, as a consequence, the appearance of rotational-like band structures is also expected. Further, it is possible to observe band termination at a comparatively low excitation energy and spin regime due to the availability of limited number of valence nucleons. Thus, the *sd*-shell nuclei such as ^{29}Al are ideal candidates to probe the possible onset of multifaceted excitation modes. This motivated us to undertake the detail investigations on the level structure of ^{29}Al using a heavy-ion induced fusion evaporation reaction. Recently, Dungan *et al.* [12] have reported results on the level structure of ^{29}Al using

*anagha.chakraborty@visva-bharati.ac.in
†Present address: TRIUMF, 4004 Wesbrook Mall, Vancouver, British Columbia, Canada V6T 2A3.

the ^{18}O(^{14}C,$p2n$) reaction at an incident beam energy of 40 MeV. Indeed, the level scheme of ^{29}Al as deduced from the present measurement is similar to that of Dungan *et al.* [12]. However, the use of a larger array in the present work, with the detectors distributed at different angles about the beam direction, facilitated observation of Doppler shapes/shifts in the γ-ray spectra. These could be successfully analyzed for level lifetime determination thanks to recent developments [13,14] pertaining to the analysis of DSAM data acquired in unconventional experimental scenarios such as the one using a thick molecular target in the present case. The determination of the level lifetimes has allowed us to classify the level sequences into two bandlike structures, wherein the levels are interconnected by strong $M1$ transitions. The possible novel features of the proposed bands are presented. The preliminary results from the present investigation have been reported previously [15].

II. EXPERIMENTAL PROCEDURE AND DATA ANALYSIS

High spin states in ^{29}Al were populated following the ^{18}O(^{13}C,1p1n)^{29}Al reaction, using a 30-MeV ^{13}C beam provided by the BARC-TIFR Pelletron Linac facility at Mumbai, India. A molecular target in the form of Ta_2O_5 was prepared by heating a thick Ta-foil (of 50 mg/cm^2 thickness) in an atmosphere of enriched ^{18}O. Considering the layers of oxygen on both sides of the Ta-foil, the total thickness of ^{18}O was estimated to be $\sim$1.6 mg/cm^2. The thick Ta-foil was *effectively* used as backing material with its thickness sufficient enough to stop the incident beam and the evaporation residues. Thus, only the front-layer of ^{18}O could contribute to the reaction process. The de-exciting γ rays were detected using Indian National Gamma Array (INGA) [16], which, at the time of the experiment, was composed of 15 Compton suppressed high-resolution clover detectors. The detectors were placed at different positions (both at the forward and backward angles), covering the angular range between 40° and 245° with respect to the beam direction. Two- and higher-fold coincidence γ events were recorded using a DSP-based data acquisition system [17]. A total of about 1.6×10^9 such coincidence events were recorded during the experiment which were subsequently sorted into the conventional $\gamma\gamma$ symmetric and angle dependent asymmetric matrices using the Linux based software package MARCOS [18]. The subsequent off-line data analysis from these matrices was carried out using the RADWARE [19] software package. A representative $\gamma\gamma$ coincidence spectrum obtained by setting the gate on the ground state feeding 1753-keV ($7/2^+_1 \rightarrow 5/2^+_1$) transition of ^{29}Al is shown in Fig. 1.

The multipolarities of the transitions belonging to ^{29}Al have been assigned following the analysis of the observed angular coincidence anisotropy. As detailed in Refs. [20,21], since the level lifetimes were comparable to the stopping time of the residues in the target/backing material, resulting in observation of angle-dependent Doppler shapes and shifts in several transitions, it was not possible to employ the conventional analysis procedure of measurement of directional correlations of γ-rays de-exciting oriented states (DCO-method) [22]. The multipolarities of the de-exciting transitions have been deduced

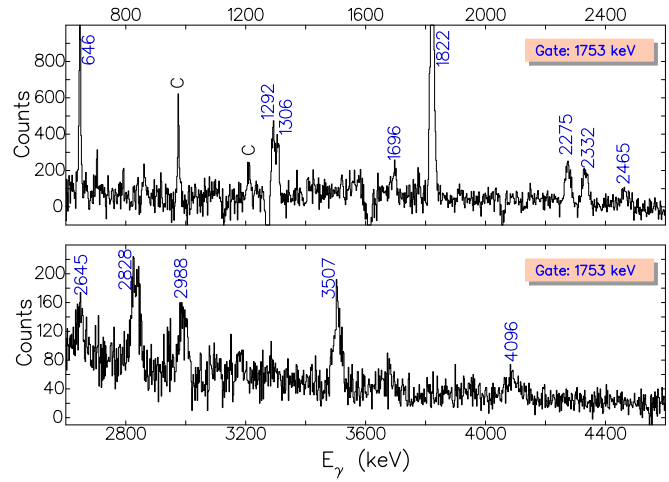

FIG. 1. The representative $\gamma\gamma$ coincidence spectrum with the gate set on the ground state feeding 1753 ($7/2^+ \rightarrow 5/2^+$)-keV transition. The spectrum has been generated using the coincidence data among the detectors at 90°. The peaks labeled with their energies belong to ^{29}Al. The contaminant transitions have been marked with "C."

from the anisotropy ratio $R_{\rm asym}$ [20,21], defined as

$$R_{\rm asym} = \frac{I_{\gamma_1} \text{ at } 40^\circ \text{ gated with } \gamma_2 \text{ at } 90^\circ}{I_{\gamma_1} \text{ at } 65^\circ \text{ gated with } \gamma_2 \text{ at } 90^\circ}.$$

To extract $R_{\rm asym}$-ratios, the coincidence data were sorted into two asymmetric matrices whose one axis corresponded to the γ-ray energy deposited in the detectors either at 40° or at 65° with respect to the beam direction and the other axis corresponded to the γ-ray energy deposited in the detectors at 90°. Polarization measurements of the de-exciting γ transitions could not be carried out because of the limited set of data in the present experiment.

III. EXPERIMENTAL RESULTS AND DISCUSSION

The relevant part of the level scheme of ^{29}Al obtained from the present work is presented in Fig. 2(a). The level scheme has been constructed using the conventional γ-γ coincidence technique. The observed regular sequences of levels have been arranged into two groups labeled Band-I and Band-II, respectively. The levels within each of these "bands" are found to be connected by strong $M1$ transitions.

The results of $R_{\rm asym}$ analysis are depicted in Fig. 3. As is evident from the figure, the 646-, 1292-, 1696-, 1753-, 1822-, 2275-, and 2332-keV transitions exhibit almost identical $R_{\rm asym} \approx 1.2$. The present measurement yields a nearly identical value for the dipole ($\Delta J = 1$), 1130-keV transition in ^{26}Mg [21]. This transition decays from the 2.9 MeV level in ^{26}Mg and has a reported mixing ratio of $|\delta| = 0.12(2)$ [23]. Hence, it may be concluded that the aforementioned transitions predominantly involve a change in angular momentum of $\Delta J = 1$. This is further supported by the reported mixing ratio ($|\delta|$) for these transitions by Beck *et al.* [5], which is suggestive of the presence of about 3%, 1%, and 0.8%-$E2$ component in the 1753-, 1822-, and 2275-keV dipole transitions of Band-I, respectively. Further, the similarity in the measured $R_{\rm asym}$

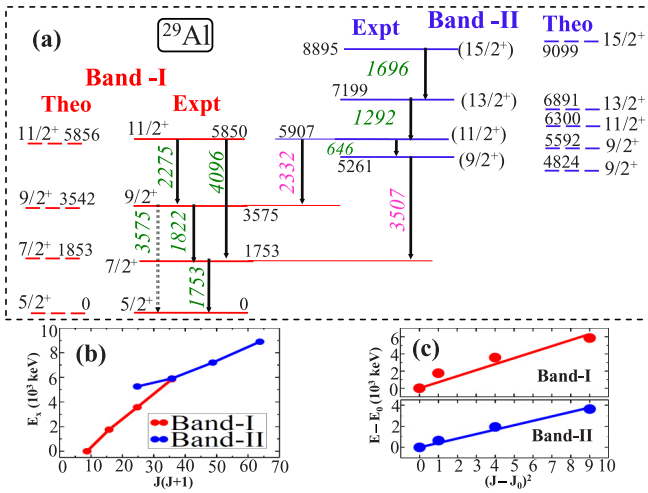

FIG. 2. (a): Partial decay scheme of ^{29}Al highlighting the two sequences (Band-I and Band-II) interconnected with strong $M1$ transitions. The predicted excitation energies from the shell model calculations are indicated by dotted levels. The variation of the excitation energy as a function of spin is presented in (b) and (c). The 3575 keV transition has not been observed in the present study. Refer text for details.

values for the 646-, 1292-, and 1696-keV transitions (members of Band-II) to the corresponding values for members of Band-I is indicative of a qualitatively similar type of electromagnetic nature for them as well. Hence, it may be surmised that the γ transitions in both these bands are associated with the presence of a very small contribution of $E2$ components.

Band-I [see Fig. 2(a)] is based on the $J^\pi = 5/2^+$ ground state, with members at E_x (in keV) $[J^\pi] = 0[5/2^+]$, 1753 $[7/2^+]$, 3575 $[9/2^+]$, and 5850 $[11/2^+]$, and has two previously reported $E2$ cross-over transitions [5], of which we have observed the 4096-keV transition; while the weaker 3575-keV cross-over transition could not be observed in the present work probably because of the lack of sufficient statistics. Further, no cross-over $E2$-transitions have been observed in Band-II

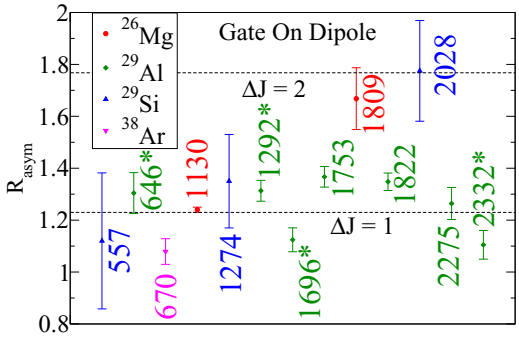

FIG. 3. The $R_{\rm asym}$ values for the transitions of present interest in ^{29}Al. The fitted values for the transitions (with known multipolarities) of a few other residual nuclei, populated in the same reaction, have also been depicted for comparison. The $\Delta J = 1$ and $\Delta J = 2$ lines have been drawn to guide the eye. The transitions belonging to Band-II of ^{29}Al have been marked with $*$.

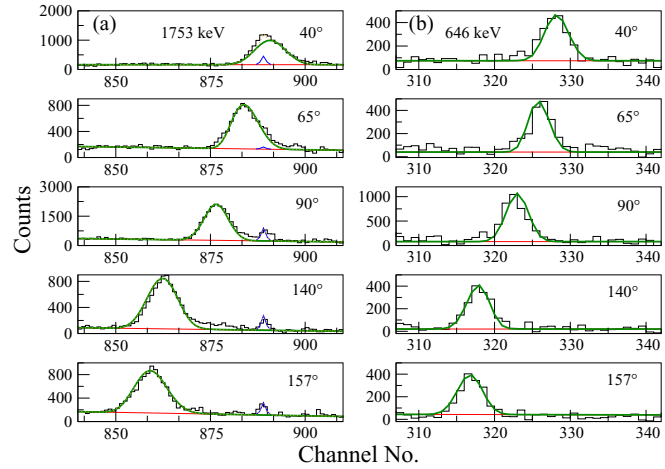

FIG. 4. Representative fits to the Doppler shapes observed for (a) 1753-keV and (b) 646-keV transitions belonging to Band-I and Band-II, respectively, of ^{29}Al. The contaminant stopped peak, as indicated in panel (a), belongs to ^{26}Mg.

[see Fig. 2(a)], which is composed of members at E_x (in keV) $[J^\pi] = 5261\,[(9/2^+)]$, 5907 $[(11/2^+)]$, 7199 $[(13/2^+)]$, and 8895 $[(15/2^+)]$. Therefore, it may be concluded that both the bands appear to be dipole bands with dominant $M1$ contributions. Band-II is found to feed into Band-I by connecting transitions of 2332 keV $[(11/2^+) \rightarrow 9/2^+]$ and 3507 keV $[(9/2^+) \rightarrow 7/2^+]$. A plot of E_x as a function of $J(J+1)$ for these bands are presented in Fig. 2(b). Qualitatively, a smooth variation in the γ-ray energy as a function of angular momentum is distinctly visible from the figure. This is suggestive of the occurrence of two rotational-like band structures in this nucleus. The difference in the slopes for the two bands possibly indicates a difference in the underlying configurations, and a crossing of the two bands appears to occur at $J = 11/2\hbar$.

Using the reported branching ratios of $M1$- and the two cross-over $E2$-transitions, by Beck *et al.* [5], we observe that Band-I has a substantial value for $\Im^{(2)}/B(E2)$ ($\Im^{(2)}$ being the dynamic moment of inertia). The values are [in units of MeV^{-1}(eb)$^{-2}$] ~28 000 and 3600, respectively, for the two cross-over transitions decaying from the 3575- and 5850-keV levels. These values are quite large in comparison with nuclei with well deformed [~10 MeV^{-1}(eb)$^{-2}$] or super deformed [~5 MeV^{-1}(eb)$^{-2}$] structures. The absence of cross-over E2-transitions did not permit us to deduce $\Im^{(2)}/B(E2)$ values for the relevant cases in Band-II. Further, if we were to plot the experimental excitation energies for Band-I and II as a function of spin, using the relation $E - E_o = A_o \times (J - J_o)^2$, where E_o and J_o corresponds to the energy and spin of the band head, a linear trend would indicate possible occurrence of shears like mechanism [24]; the same is observed in case of both bands [see Fig. 2(c)].

Thus, these bands provide hints of "magnetic rotation (MR)" like band structure in this nucleus even in the absence of any high-j orbitals. This is further corroborated by the associated $B(M1)$ transition probabilities, which could be deduced following the measurements of level lifetimes. These

TABLE I. The values of mean lifetime (τ, in fs) of the levels of ^{29}Al obtained from the present measurement. The quoted uncertainties are obtained from χ^2 minimization analysis. The quoted lifetime values do not include stopping power uncertainties which is ∼5%. The reported level lifetimes from the previous measurements [6,7] have also been incorporated for comparison. The quoted experimental $B(M1)$ values have been obtained using the lifetime values of the concerned levels extracted from the present measurement.

	J^π	E_x (keV)	E_γ (keV)	τ_{present} (fs)	τ [6] (fs)	τ [7] (fs)	$B(M1)$ (μ_N^2)
Band-I	$7/2^+$	1753.3(9)	1752.7(10)	18 ± 2	25 ± 11	80 ± 40	0.57^{+8}_{-6}
	$9/2^+$	3575.2(13)	1822.1(10)	16^{+6}_{-5}	36 ± 10	<70	0.53^{+25}_{-15}
	$11/2^+$	5849.8(18)	2274.7(20)	<166[a]	42 ± 19[c]		>0.02
Band-II	$(11/2^+)$	5906.6(18)[b]	2332.2(20)	72 ± 2			
			645.9(10)	92 ± 2			1.13^{+27}_{-25}
	$(13/2^+)$	7199.0(21)	1292.4(10)	<82[d]			>0.32
	$(15/2^+)$	8895.3(23)	1696.3(10)	<68[a]			>0.14
		5260.5(18)	3506.5(20)	171^{+7}_{-6}	110 ± 70		
		6403.3(25)	2828.1(21)	<72			

[a]An upper limit for the lifetime value of the level could only be obtained due to the presence of dominant side-feeding.
[b]Unweighted average of the lifetime values obtained from the two decay branches gives a lifetime value of 82 ± 2 fs and the quoted $B(M1)$ value is obtained using this value of level lifetime.
[c]Assuming the feeding time for the 5849-keV, $11/2^+$ level to be the same as that for the 5906-keV, $(11/2^+)$ level, a value of 42 ± 10 fs has been obtained from the present measurement for the 5849-keV, $11/2^+$ level.
[d]Only an upper limit for level lifetime could be obtained due to the lack of sufficient statistics.

lifetimes have been measured using the DSAM. The use of a thick molecular target, which is in sharp variance with the use of traditional thin-target with a high-Z elemental backing, has necessitated modification of the analysis methodology as detailed in Refs. [13,14]. The observed Doppler shapes and shifts of the de-exciting γ-ray from the concerned level have been fitted simultaneously at 40°, 65°, 90°, 140°, and 157° and the corresponding level lifetime was extracted. A representative plot showing the fits to the observed Doppler shapes for the 1753- and 646-keV transitions decaying from the 1753- and 5907-keV levels (members of Band-I and Band-II), respectively, is presented in Fig. 4. The level lifetimes obtained from the present measurements have been summarized in Table I. The use of SRIM-updated stopping powers has narrowed down the uncertainties in the stopping simulations to ⩽5%, which have not been included in the quoted uncertainties.

The extracted level-lifetimes were subsequently used to obtain the reduced transition probabilities $B(M1)$ for both the bands, which are presented in Fig. 5. For the transitions de-exciting the levels in Band I, the $B(M1)$ values were determined by using the mixing and branching ratio values from Ref. [5]. The $B(M1)$ values for the transitions of Band-II were extracted using the predicted mixing-ratio values (which are small in magnitude) from shell model calculations (discussed later in the text). However, similar results are obtained by considering the transitions to be pure $M1$ in nature. If one were to collate the present and previously reported lifetime values for Band-I, and deduce the transition probabilities therefrom, a qualitatively similar decreasing trend is observed as presented in Fig. 5. This decreasing trend for $B(M1)$ values as a function of spin is considered to be a necessary signature for MR band [24,25]. A similar, though not identical, decreasing trend of $B(M1)$ values hold for Band-II as well.

It is to be noted here that more than 130 magnetic rotational bands have been identified so far in five distinct mass regions across the nuclear landscape near A ≈ 190, A ≈ 140, A ≈ 110, A ≈ 80, and A ≈ 60 [26–28]. This phenomenon has not yet been observed in any nuclei with A ⩽40. The excitation of nucleons from the $d_{5/2}$ into the $d_{3/2}$ orbital, the

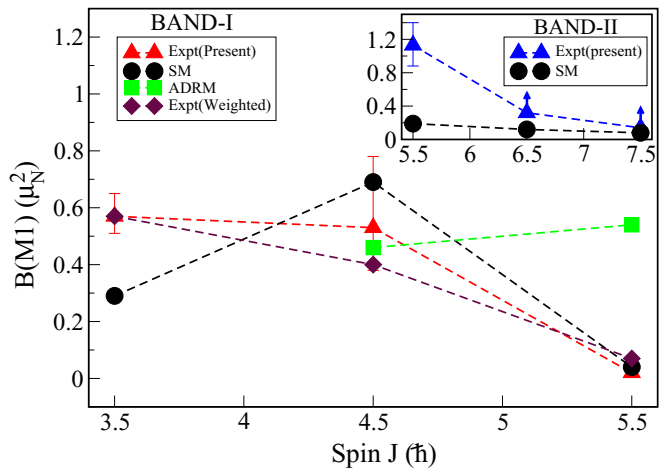

FIG. 5. The variation of experimental and theoretical $B(M1)$ values for the transitions belonging to Band-I and Band-II of ^{29}Al as a function of angular momentum. The experimental $B(M1)$ values from the present measurement [Expt(Present)] and those obtained using the weighted average value of level lifetime considering the present and the past measurement [6] [Expt(Weighted)] are shown. The predicted results from the shell model calculation [SM] are also plotted for comparison. It is obvious that the constant nature of $B(M1)$ values as per the prediction from the axially deformed rotor model [ADRM] [31] is in sharp contrast to that of the experimentally observed trend.

TABLE II. $(g_K - g_R)$ values for the transitions belonging to Band-I of ^{29}Al and the corresponding $B(M1)$ transition rates.

J^π	E_x (keV)	E_γ (keV)	$(g_K - g_R)_{\text{Expt}}$[d]	Nilsson configuration: $(g_K - g_R)_{\text{theory}}$[e,f]	$B(M1)_{\text{theory}}$[g] (μ_N^2)	$B(M1)_{[6]}$ (μ_N^2)	$B(M1)_{\text{present}}$ (μ_N^2)
$9/2^+$	3575	1822.1[b]	1.00 ± 0.23	$5/2^+[202]$: 1.0	0.46	$0.24^{+0.09}_{-0.06}$	0.57^{+8}_{-6}
$11/2^+$	5850	2274.7[b]	1.13 ± 0.40		0.54	$0.07^{+0.07}_{-0.02}$	>0.02
$(13/2^+)$	7263[a]	1411[c]	0.53 ± 0.17		0.59		

[a]This level is not observed from the present investigation and has been taken from the work of Dungan *et al.* [12].
[b]δ value for the decay branch has been taken from Ref. [5].
[c]δ value for the decay branch is not available; a value of $\delta = 0.10 \pm 0.03$ has been assumed in extracting the corresponding value of $(g_K - g_R)_{\text{Expt}}$.
[d]Extracted using $Q = Q_0 = +0.26(3)$ eb for ^{26}Al [39].
[e]Extracted following the procedure as mentioned in Ref. [37].
[f]A value of $g_R = Z/A = 0.45$ has been used for the calculation.
[g]The $B(M1)$ values have been calculated using the relation [40]

$$B(M1) = \frac{3}{4\pi}\mu_N^2 (g_K - g_R)^2 K^2 \frac{(I-K)(I+K)}{I(2I+1)}. \tag{3}$$

The theoretical $(g_K - g_R)$ value has been used for the calculation.

highest available j orbitals within the sd-shell region, may provide conditions conducive for the occurrence of MR-like sequences in this region and the possibility for the observation of this phenomenon in this region cannot be ruled out as there exists prediction for the occurrence of a magnetic rotational band in an even lighter-mass nucleus, ^{22}F [29]. The $B(M1)$ values for the transitions of Band-I are typically $<1\,\mu_N^2$ and those for Band-II are typically $<2\,\mu_N^2$. These strengths are somewhat lower in comparison with those for the MR-bands observed in higher mass regions [24,25,30]; this is possibly because of the unavailability of high-j proton orbitals. All the previously observed MR bands in higher-mass regions are based on configurations involving high-j proton orbitals such as $g_{9/2}$ (in $A \approx 80$ and 100–110 regions), $h_{9/2}$ (in $A \approx 140$ region), and $h_{9/2}, i_{13/2}$ (in $A \approx 200$ region). The involvement of these high-j proton configurations gives rise to higher values of $B(M1)$, typically of the order of 2–10 μ_N^2.

Band-I was previously identified by Jones *et al.* [32] as a $K^\pi = 5/2^+$ band. If one were to assume that this proposition is valid, then the expected feature for an axially deformed nucleus is a constant, or an increasing trend of the $B(M1)$ values as function of spin [33], which is at a sharp variance with the present observations. However, in the neighboring odd-mass Al-isotopes (^{25,27}Al) where such $K^\pi = 5/2^+$ bands are observed [32,34–36], the corresponding $B(M1)$ values show either a constant or an increasing trend as a function of spin, corroborating a pure axially deformed-rotor-like behavior. For an axially deformed nucleus, the sign of the mixing ratio (δ) for an in-band dipole transition determines the nature of deformation (prolate or oblate). Ekstrom *et al.* [6] have reported a negative sign for the measured mixing ratio values for the members of Band-I. As is evident from the equations [6,37]

$$\frac{|g_K - g_R|}{Q_0} = \frac{0.93 E_\gamma}{\delta\sqrt{I^2 - 1}}, \tag{1}$$

$$\text{sgn}(\delta) = -\text{sgn}\left(\frac{g_K - g_R}{Q_0}\right), \tag{2}$$

a negative value for δ would result in a positive value of Q_0, assuming a positive value for $(g_K - g_R)$ (see Table II). Hence, the ground-state structure of ^{29}Al is concluded to be prolate in nature.

It is to be pointed out here that even with the limited spectroscopic information available in the present work, it is possible to draw conclusions, or conjecture about, presence of several interesting nuclear structure features in this nucleus:

(1) A comparison between the experimental and theoretical $(g_K - g_R)$ values for the transitions belonging to Band-I of ^{29}Al and the corresponding $B(M1)$ transition rates is presented in Table II. The value of $(g_K - g_R)_{\text{Expt}}$ for the $J^\pi = (13/2^+)$ level exhibits a sharp deviation from that of the nearly constant value for the lower two members. This observation is suggestive of a possible structural change in this spin domain.

(2) The theoretical branching ratios for a pair of transitions, de-exciting from the same level, of Band-I of ^{29}Al were deduced following the Alaga rule [38] and are compared with the corresponding experimental values in Table III. From the table, it can be seen that the comparison between the experimental and theoretical branchings is reasonable only for the transitions decaying from the lowest two members, and a variance similar in nature to that observed in the $(g_K - g_R)$ values is noted for the $J^\pi = (13/2^+)$ level. From this observation, one might conjecture that this may be indicative of a structural change in Band-I which is approaching the terminating state at $J^\pi = (13/2^+)$ wherein the onset of other single-particle excitations results in K no longer remaining a good quantum number.

(3) The decreasing trend for $B(E2)$ values is an important experimental indicator for a band approaching the terminating state. However, within the present experimental data set, it is not possible to address the issue because of the presence of large uncertainties in the deduced $B(E2)$ values for the $E2$ transitions in

TABLE III. Comparison between the experimental and predicted (following the Alaga rule) branching ratios (BR) for the transitions belonging to Band-I of ^{29}Al.

E_x (keV)	E_γ (keV)	$J_i^\pi \rightarrow J_f^\pi$	BR_{expt}	BR_{Alaga}
3575	1822.1	$9/2^+ \rightarrow 7/2^+$	100(1)	100
	3575[a]	$9/2^+ \rightarrow 5/2^+$	10(1)	33
5850	2274.7	$11/2^+ \rightarrow 9/2^+$	100(3)	100
	4096.3	$11/2^+ \rightarrow 7/2^+$	54(3)	47
7263	1411[b]	$(13/2^+) \rightarrow 11/2^+$	100(25)	100
	3688[b]	$(13/2^+) \rightarrow 9/2^+$	100(25)	55

[a]This decay branch is not observed in the present investigation due to lack of statistics in the present experimental data; the adopted branching from Ref. [5] is considered.
[b]This decay branch is not observed in the present investigation and has been taken from the work of Dungan *et al.* [12].

Band-I. The major source of these uncertainties may be attributed to the associated uncertainties with the deduced $E2$ branchings.

Based on the above discussions, it may be surmised that there is a possibility of a confluence of competing excitation modes in Band-I.

Detailed shell model calculations have been carried out using the shell-model code NuShellX@MSU [41]. The calculations were performed with a model space consisting of $1d_{5/2}$, $2s_{1/2}$, and $1d_{3/2}$ orbitals outside the ^{16}O core. The "*usda*" effective interaction [41] has been used for this "*sd*" model space. The calculations have been carried out without imposing any restrictions on the occupancies of the valence particles in the available valence space. The predicted excitation energies are found to be in excellent agreement with the experimental observations for the members of Band-I, with the maximum deviation between the experimental and theoretical level energies about 100 keV [see Fig. 2(a)]; for Band-II, the maximum deviation is about 400 keV. The ordering of the experimental levels belonging to both the bands is reproduced by the calculations, which suggest that the most dominant wave functions of the members of the two bands are: $\pi[d_{5/2}^{-2}(s_{1/2}d_{3/2})^1] \otimes \nu[d_{5/2}^{-1}(s_{1/2}d_{3/2})^3]$ (for Band-I) and $\pi[d_{5/2}^{-2}(s_{1/2}d_{3/2})^1] \otimes \nu[d_{5/2}^{-1}s_{1/2}^1 d_{3/2}^2]$ (for Band-II). The effective charges and the g-factors that have been used for the calculations of electromagnetic transition probabilities are the same as those used previously to predict the spectroscopic properties of the neighboring sd-shell nuclei [42]. The comparison between the experimental and theoretical values of the electromagnetic transition probabilities is presented in Fig. 5. As is evident from the figure, the model predictions for the transition probabilities are in qualitative agreement with the experimental trends. Considering the most dominating configuration for Band-I, the maximum spin that can be generated is $13/2^+$ $(\pi[d_{5/2(J=0)}^{-2}(s_{1/2}d_{3/2})^1_{(J=3/2)}]_{J=3/2} \otimes \nu[d_{5/2(J=5/2)}^{-1}(s_{1/2}d_{3/2})^3_{(J=5/2)}]_{J=10/2})$. As mentioned earlier (see Table III), Dungan *et al.* [12] placed a level at E_x = 7263 keV, which decays to the lower level members of Band-I through 1411- and 3688-keV transitions. From the present study, it is not possible to place the level in the level scheme because of the limited statistics in our data. However, the decay branches placed by Dungan *et al.* [12] are suggestive of probable $(13/2^+)$ spin for this level. This leads to the possible conclusion that Band-I terminates at E_x = 7263 keV with $J^\pi = (13/2^+)$.

As mentioned earlier, the deformation of the two bands is not similar. This is reflected in the level spacing between the two lower most levels of the corresponding bands. The excited band (Band-II) appears to be more deformed than the ground state band (Band-I). However, the presence of the enhanced deformation for the excited band could not hinder the decreasing nature of the $B(M1)$ values as function of spins (see Fig. 5). This is contrary to what has been observed in other mass regions where the $B(M1)$ values appear to remain constant over an extended spin regime because of the effect of enhanced deformation [43]. As can be seen from Table II, the axially deformed rotor model could predict very well the experimental $B(M1)$ values at lower-most excitation; but it fails to reproduce the decreasing trend of $B(M1)$ values with increasing spin (see Fig. 5).

IV. CONCLUSIONS

The present work reports the spectroscopic results on the nucleus ^{29}Al, following population via heavy-ion induced fusion evaporation reaction. Two separate sequences of levels, Band-I and Band-II, are identified. The measurement of the level lifetimes, and the deduced transition probabilities therefrom, reveal that both the sequences satisfy the expected experimental indicators for magnetic-rotation-like behavior even in the absence of any high-j orbital. This is contrary to the occurrence of "magnetic rotation" bands observed in higher mass region where the high-j orbitals, in general, play the role of shears formation. The shell model calculations reproduce the experimental results reasonably well. Evidence for the possible termination of the prolate deformed ground state band (Band-I) is also presented. The present experimental data is suggestive of multiple heterogeneous excitation mechanisms contributing to the observed level structure and demands further experimental and theoretical investigations.

ACKNOWLEDGMENTS

This work has been carried out as a part of the Collaborative Research Scheme (CRS) of UGC-DAE CSR, Kolkata (Ref. No. UGC-DAE-CSR-KC/CRS/13/NP04/). The help and cooperation received from all the participants for their joint effort in setting up the INGA facility at TIFR is deeply acknowledged. Thanks also due to the staff of the BARC-TIFR Pelletron Linac Accelerator facility for their support during the experiment. This work has been supported in part by the U.S. National Science Foundation (Grant No. PHY-1713857). Financial support from the Department of Science and Technology (D.S.T.), Government of India (Grant No. IR/S2/PF-03/2003-II) is also gratefully acknowledged.

[1] D. R. Goosman, C. N. Davids, and D. E. Alburger, Phys. Rev. C **8**, 1331 (1973).
[2] C. Détraz, D. Guillemaud, G. Huber, R. Klapisch, M. Langevin, F. Naulin, C. Thibault, L. C. Carraz, and F. Touchard, Phys. Rev. C **19**, 164 (1979).
[3] D. Guillemaud-Mueller *et al.*, Nucl. Phys. A **426**, 37 (1984).
[4] J. R. Williams, R. O. Nelson, C. R. Gould, and D. R. Tilley, Phys. Rev. C **11**, 1111 (1975).
[5] F. A. Beck, T. Byrski, A. Knipper, and J. P. Vivien, Phys. Rev. C **13**, 1792 (1976).
[6] P. Ekström and J. Tillman, Nucl. Phys. A **230**, 285 (1974).
[7] F. A. Beck, T. Byrski, G. Costa, and P. Engelstein, Nucl. Phys. A **218**, 213 (1974).
[8] M. J. A. De Voigt, P. W. M. Glaudemans, J. De Boer, and B. H. Wildenthal, Nucl. Phys. A **186**, 365 (1972).
[9] M. J. A. De Voigt and B. H. Wildenthal, Nucl. Phys. A **206**, 305 (1973).
[10] A. D. W. Jones, Phy. Rev. **180**, 997 (1969).
[11] H. Mackh, G. Mairle, and G. J. Wagner, Z. Phys. **269**, 353 (1974).
[12] R. Dungan, S. L. Tabor, R. S. Lubna, A. Volya, V. Tripathi, B. Abromeit, D. D. Caussyn, K. Kravvaris, and P.-L. Tai, Phys. Rev. C **94**, 064305 (2016).
[13] R. Bhattacharjee, S. S. Bhattacharjee, K. Basu, P. V. Rajesh, R. Raut, S. S. Ghugre, D. Das, A. K. Sinha, L. Chaturvedi, U. Garg, S. Ray, B. K. Yogi, M. K. Raju, R. Chakrabarti, S. Mukhopadhyay, A. Dhal, R. P. Singh, N. Madhavan, and S. Muralithar, Phys. Rev. C **90**, 044319 (2014).
[14] S. Das *et al.*, Nucl. Instrum. Methods Phys. Res. A **841**, 17 (2017).
[15] H. Sultana *et al.*, in *Proceedings of the 61st DAE-BRNS Symposium on Nuclear Physics*, Kolkata, India, 2016, edited by B. V. John, D. Dutta, and A. Saxena, Vol. 61 (2016), p. 192.
[16] N. Rather, P. Datta, S. Chattopadhyay, S. Rajbanshi, A. Goswami, G. H. Bhat, J. A. Sheikh, S. Roy, R. Palit, S. Pal, S. Saha, J. Sethi, S. Biswas, P. Singh, and H. C. Jain, Phys. Rev. Lett. **112**, 202503 (2014).
[17] R. Palit *et al.*, Nucl. Instrum. Methods Phys. Res. A **680**, 90 (2012).
[18] S. Saha, R. Palit, J. Sethi, T. Trivedi, P. C. Srivastava, S. Kumar, B. S. Naidu, R. Donthi, S. Jadhav, D. C. Biswas, U. Garg, A. Goswami, H. C. Jain, P. K. Joshi, G. Mukherjee, Z. Naik, S. Nag, V. Nanal, R. G. Pillay, S. Saha, and A. K. Singh, Phys. Rev. C **86**, 034315 (2012).
[19] D. C. Radford, Nucl. Instrum. Methods Phys. Res. A **361**, 297 (1995).
[20] R. Chakrabarti, S. Mukhopadhyay, R. Bhattacharjee, S. S. Ghugre, A. K. Sinha, A. Dhal, L. Chaturvedi, M. K. Raju, N. Madhavan, R. P. Singh, S. Muralithar, B. K. Yogi, and U. Garg, Phys. Rev. C **84**, 054325 (2011).
[21] S. S. Bhattacharjee, R. Bhattacharjee, R. Chakrabarti, R. Raut, S. S. Ghugre, A. K. Sinha, T. Trivedi, L. Chaturvedi, S. Saha, J. Sethi, and R. Palit, Phys. Rev. C **89**, 024324 (2014).
[22] A. Krämer-Flecken *et al.*, Nucl. Instrum. Methods Phys. Res. A **275**, 333 (1989).
[23] C. Broude and H. E. Gove, Ann. Phys. (NY) **23**, 71 (1963).
[24] R. M. Clark, S. J. Asztalos, B. Busse, C. J. Chiara, M. Cromaz, M. A. Deleplanque, R. M. Diamond, P. Fallon, D. B. Fossan, D. G. Jenkins, S. Juutinen, N. Kelsall, R. Krucken, G. J. Lane, I. Y. Lee, A. O. Macchiavelli, R. W. MacLeod, G. Schmid, J. M. Sears, J. F. Smith, F. S. Stephens, K. Vetter, R. Wadsworth, and S. Frauendorf, Phys. Rev. Lett. **82**, 3220 (1999).
[25] R. M. Clark and A. O. Macchiavelli, Annu. Rev. Nucl. Part. Sci **50**, 1 (2000).
[26] D. A. Torres, F. Cristancho, L.-L. Andersson, E. K. Johansson, D. Rudolph, C. Fahlander, J. Ekman, R. duRietz, C. Andreoiu, M. P. Carpenter, D. Seweryniak, S. Zhu, R. J. Charity, C. J. Chiara, C. Hoel, O. L. Pechenaya, W. Reviol, D. G. Sarantites, L. G. Sobotka, C. Baktash, C.-H. Yu, B. G. Carlsson, and I. Ragnarsson, Phys. Rev. C **78**, 054318 (2008).
[27] D. Steppenbeck, R.V.F. Janssens, S. J. Freeman, M. P. Carpenter, P. Chowdhury, A. N. Deacon, M. Honma, H. Jin, T. Lauritsen, C. J. Lister, J. Meng, J. Peng, D. Seweryniak, J. F. Smith, Y. Sun, S. L. Tabor, B. J. Varley, Y.-C. Yang, S. Q. Zhang, P. W. Zhao, and S. Zhu, Phys. Rev. C **85**, 044316 (2012).
[28] P. W. Zhao *et al.*, Phys. Lett. B **699**, 181 (2011).
[29] P. Jing *et al.*, Chin. Phys. Lett. **27**, 122101 (2010).
[30] D. Choudhury *et al.*, Phys. Rev. C **91**, 014318 (2015).
[31] W. Greiner and J. A. Maruhn, *Nuclear Models* (Springer-Verlag, Berlin Heidelberg, 1996).
[32] A. D. W. Jones, J. A. Becker, and R. E. McDonald, Phys. Rev. C **3**, 724 (1971).
[33] F. Dönau and S. Frauendorf, in *Proceedings of the International Conference on High Angular Momentum Properties of Nuclei, Oak Ridge, 1982*, edited by N. R. Johnson (Harwood Academic, New York, 1983), p. 143.
[34] R. B. Firestone, Nucl. Data Sheets **110**, 1691 (2009).
[35] M. Shamsuzzoha Basunia, Nucl. Data Sheets **112**, 1875 (2011).
[36] Data retrieved from the Evaluated Nuclear Structure Data File (ENSDF) available at www.nndc.bnl.gov/ensdf/ for ^{25}Al (updated on 11 December 2013).
[37] P. H. Regan, G. D. Dracoulis, A. P. Byrne, G. J. Lane, T. Kibédi, P. M. Walker, and A. M. Bruce, Phys. Rev. C **51**, 1745 (1995).
[38] G. Alaga, K. Alder, A. Bohr, and B. R. Mottelson, K. Dan. Vidensk. Selesk. Mat. Fys. Medd. **29**, 1 (1955).
[39] N. J. Stone, At. Data Nucl. Data Tables, **111-112**, 1 (2016).
[40] P. Ring and R. Schuck, *The Nuclear Many Body Problem* (Springer-Verlag, New York, 1980).
[41] NushellX@MSU, B. A. Brown and W. D. M. Rae, MSU-NSCL Report 524:1-29 (2007).
[42] W. A. Richter, S. Mkhize, and B. A. Brown, Phys. Rev. C **78**, 064302 (2008).
[43] A. O. Evans *et al.*, Phys. Lett. B **636**, 25 (2006).